HHS Public Access

Author manuscript

Anal Chem. Author manuscript; available in PMC 2024 June 20.

Published in final edited form as:

Anal Chem. 2023 June 20; 95(24): 9347–9356. doi:10.1021/acs.analchem.3c01426.

The Added Value of Internal Fragments for Top-down Mass Spectrometry of Intact Monoclonal Antibodies and Antibody-Drug Conjugates

Benqian Wei[1], **Carter Lantz**[1], **Weijing Liu**[5], **Rosa Viner**[5], **Rachel R. Ogorzalek Loo**[1,3,4], **Iain D. G. Campuzano**[6], **Joseph A. Loo**[1,2,3,4,*]

[1]Department of Chemistry and Biochemistry, University of California Los Angeles-Los Angeles, CA, 90095 USA

[2]Department of Biological Chemistry, University of California-Los Angeles, Los Angeles, CA, 90095 USA

[3]UCLA-DOE Institute, University of California-Los Angeles, Los Angeles, CA, 90095 USA

[4]Molecular Biology Institute, University of California-Los Angeles, Los Angeles, CA, 90095 USA

[5]Thermo Fisher Scientific, San Jose, CA, 95134 USA

[6]Amgen Research, Center for Research Acceleration and Digital Innovation, Molecular Analytics, Thousand Oaks, CA, 91320 USA

Abstract

Monoclonal antibodies (mAbs) and antibody-drug conjugates (ADCs) are two of the most important therapeutic drug classes that require extensive characterization, whereas their large size and structural complexity make them challenging to characterize and demand the use of advanced analytical methods. Top-down mass spectrometry (TD-MS) is an emerging technique that minimizes sample preparation and preserves endogenous post-translational modifications (PTMs); however, TD-MS of large proteins suffers from low fragmentation efficiency, limiting the sequence and structure information that can be obtained. Here, we show that including the

[*]**Corresponding Author**: **Joseph A. Loo** – Department of Chemistry and Biochemistry, University of California Los Angeles, Los Angeles, California 90095, United States; JLoo@chem.ucla.edu.

Authors

Benqian Wei – Department of Chemistry and Biochemistry, University of California Los Angeles, Los Angeles, California 90095, United States

Carter Lantz – Department of Chemistry and Biochemistry, University of California, Los Angeles, Los Angeles, California 90095, United States

Weijing Liu – Thermo Fisher Scientific, San Jose, California 95134, United States

Rosa Viner – Thermo Fisher Scientific, San Jose, California 95134, United States

Rachel R. Ogorzalek Loo – Department of Chemistry and Biochemistry, University of California, Los Angeles, Los Angeles, California 90095, United States

Iain D. G. Campuzano – Amgen Research, Center for Research Acceleration and Digital Innovation, Molecular Analytics, Biologics Therapeutic Discovery, Thousand Oaks, California 91320, United States

Supporting Information

The Supporting Information is available free of charge on the ACS Publications website.

The conjugation process of the ADC; additional native MS, deconvoluted, and representative ECD MS/MS spectra; additional fragment location maps showing the identification of N-glycosylation identification; additional data showing the exact values of sequence coverage and number of drug conjugation sites; and instrument and ExD cell parameters.

The authors declare no competing financial interest.

assignment of internal fragments in native TD-MS of intact mAbs and ADCs can improve their molecular characterization. For the NIST mAb, internal fragments can access the sequence region constrained by disulfide bonds to increase the TD-MS sequence coverage to over 75%. Important PTM information, including intra-chain disulfide connectivity and N-glycosylation sites, can be revealed after including internal fragments. For a heterogenous lysine-linked ADC, we show that assigning internal fragments improves the identification of drug conjugation sites to achieve a coverage of 58% of all putative conjugation sites. This proof-of-principle study demonstrates the value of including internal fragments in native TD-MS of intact mAbs and ADCs, and this analytical strategy can be extended to bottom-up and middle-down MS approaches to achieve even more comprehensive characterization of important therapeutic molecules.

INTRODUCTION

Monoclonal antibody (mAb) therapeutics have become increasingly important for the diagnosis and treatment of a host of diseases including cancer and viral infections. They can achieve targeted tumor cell elimination with high specificity and desirable pharmacokinetics properties.[1–7] MAbs are highly complex molecules with large size (~150 kDa), and have a series of intra- and inter-chain disulfide bridges and numerous post-translational modifications (PTMs), with the most common ones being N-glycosylation, N-terminal pyroglutamine cyclization, oxidation, C-terminal lysine processing, and deamidation.[8–9] This high molecular complexity can impact critical quality attributes (CQAs)[10] of mAb products including stability, solubility, and pharmacokinetics/pharmacodynamics properties, thus extensive sequence and structure characterization are required to produce high quality mAb products.[11]

Antibody-drug conjugates (ADCs), which arm the antibodies with highly potent cytotoxic payloads via a linker to improve its antitumor efficacy, have emerged as a promising therapeutic drug class.[12–16] The conjugation of a linker and a payload onto antibodies introduces an additional dimension of heterogeneity to ADCs, increasing the challenge of their complete characterization. This is particularly true for non-specific lysine-linked ADCs, in which payloads are conjugated with primary amines (lysines and N-termini) of the antibody, resulting in a highly heterogeneous molecule with various numbers of payloads binding to a large array of locations.[12, 17–21] Comprehensive analytical profiling of ADCs include evaluating CQAs such as drug-to-antibody ratio (DAR), drug distribution, and drug conjugation sites.[22–30] In contrast to the routinely characterized DAR and drug distribution, relatively few studies have focused on determining the sites of drug conjugation sites, despite their important role in affecting the physical and pharmaceutical properties of ADCs.[17, 26, 31–32] For example, the binding specificity of lysine-linked ADCs to the target antigen can be affected if the conjugation occurs in the complementarity-determining regions (CDRs).[12, 17, 33] Such instances necessitate the determination of drug conjugation sites, particularly for non-specific lysine-linked ADCs.

Mass spectrometry (MS) based techniques, such as bottom-up MS (BU-MS) and middle-down MS (MD-MS), are powerful analytical tools routinely used for the characterization of mAbs and ADCs. BU-MS, or peptide mapping, analyzes enzymatically digested peptides of

mAbs/ADCs using liquid chromatography-tandem mass spectrometry (LC-MS/MS).[12, 34–39] While BU-MS can provide high sequence coverage with amino acid resolution and pinpoint ADC drug conjugation sites (by identifying payload-bound peptide ions), it comes at a cost of relatively extensive sample preparation and the possibility of introducing artificial PTMs.[40–42] MD-MS, which analyzes ~25 kDa subunits of mAbs and ADCs by reducing disulfide bonds and the hinge region of the antibody heavy chain, has become a promising complementary approach to BU-MS.[43–50] MD-MS does not reach the extensiveness of BU-MS in terms of sequence and drug conjugation site coverage, it avoids the digestion step required by BU-MS, although enzymatic and chemical reduction, and chromatographic separation are still necessary.

Top-down MS (TD-MS), where intact gas-phase protein ions are measured and fragmented, has gained popularity in recent years for the characterization of mAbs.[43, 51–56] Compared to BU-MS and MD-MS, TD-MS holds the advantages of minimal sample preparation and preserving endogenous modifications of mAbs. However, TD-MS suffers from low fragmentation efficiency for proteins of the size of mAbs and for proteins with significant disulfide bond compositions.[53–54, 57–58] Recently, the Coon lab utilized activated ion electron transfer dissociation (AI-ETD), a novel fragmentation technique that combines the advantage of electron- and photon-based fragmentation, to achieve over 60% sequence coverage on intact NIST mAb by TD-MS alone.[54] Although this is a substantial improvement over previous TD-MS studies, comprehensive TD-MS sequence coverage on intact mAbs is still challenging. Studies utilizing TD-MS to identify drug conjugation sites of intact ADCs are even more sparse. The Ge lab applied a three-tier TD-MS strategy for multi-attribute analysis of a site-specific cysteine-linked ADC; however, limited sequence and drug conjugation sites information are obtained due to relatively low fragmentation efficiency.[59] Thus far, BU-MS and MD-MS are still the preferred methods for the characterization of either cysteine-linked ADCs[22, 48–50, 60] or lysine-linked ADCs.[12, 17, 35, 37, 47]

A strategy to improve the apparent fragmentation efficiency of TD-MS, and thereby increase sequence information content, is to incorporate non-canonical *internal* fragments, which contain neither the N- nor C-terminus of the protein sequence, into data analysis workflow.[61] Previous studies have shown that including internal fragments in TD-MS can enhance the sequence information obtained from intact proteins,[62–67] protein complexes,[68–69] and on a proteome-wide scale.[70] Specifically, internal fragments have been demonstrated to aid the TD-MS characterization of disulfide-intact proteins,[64, 67, 71] inspiring us to investigate the application of internal fragments in TD-MS of mAbs and ADCs, which contain a large number of disulfide bonds.

Here, we show that assigning internal fragments in TD-MS increases mAb sequence coverage to over 75% and allows the determination of intra-chain disulfide connectivity and various N-glycosylation types. For a therapeutic non-specific lysine-linked ADC, identification of nearly 60% of all putative drug conjugation sites was achieved. To our knowledge, the sequence coverage reported here on intact mAbs is the highest achieved by TD-MS alone, and this is the first report utilizing TD-MS to characterize lysine-linked ADCs.

EXPERIMENTAL SECTION

Materials and Sample Preparation.

The humanized IgG1k monoclonal antibody reference material 8671 was purchased from the National Institute of Standards and Technology (NIST, Gaithersburg, MD). The naked IgG1 mAb used for ADC preparation was produced at Amgen (Thousand Oaks, CA) and comprises of two human heavy chains and two human λ light chains. The mAb was expressed in Chinese hamster ovary cells and was purified by chromatographic procedures developed at Amgen.[72] Detailed procedures for the preparation of the ADC have been described previously.[12] Briefly, a maytansinoid DM1 payload was conjugated onto primary amines of the naked IgG1 mAb through a noncleavable linker, N-succinimidyl 4-(N-maleimidomethyl)cyclohexane-1-carboxylate (SMCC) (Figure S1). Ammonium acetate solution (7.5 M) was purchased from Sigma-Aldrich (St. Louis, MO, USA) and diluted to 200 mM. The NIST mAb and ADC samples were buffer exchanged into 200 mM ammonium acetate using Biospin 6 columns (Bio-Rad) and diluted to a final concentration of 5 μM prior to native mass spectrometry measurements.

Native Top-Down Mass Spectrometry.

All samples were injected into a Thermo Q Exactive Plus UHMR Orbitrap instrument (Thermo Fisher Scientific, Bremen, Germany) modified with an electromagnetostatic ExD cell (e-MSion Inc., Corvallis, OR) located between the quadrupole and C-Trap. All protein solutions were loaded into in-house pulled capillaries coated with platinum, and electrosprayed by applying a capillary voltage between 1.1 and 1.7 kV on the NSI source. The source temperature was set at 250 °C, and the S-lens RF level was set at 200. Other crucial instrument parameters corresponding to ion transmission were listed in Table S1. For HCD fragmentation, five individual charge states of NIST mAb (22+ to 26+) and four individual ions of ADC (DAR 1 ions at charge states 23+ and 24+, DAR 2 ions at charge states 23+ and 24+) were isolated in the quadrupole, with an isolation window of 40 *m/z* before fragmentation. HCD was performed by applying CE ranging from 190V to 240V to achieve optimal fragmentation. For ECD fragmentation, the aforementioned five NIST mAb ions and four ADC ions were still isolated with an isolation window of 40 *m/z* in the quadrupole, while two additional ADC ions, DAR 1 and DAR 2 ions grouped together at charge states 22+ and 25+, were isolated with an isolation window of 80 *m/z* in the quadrupole due to lower signal level of these two charge states. After isolation, these ions were transmitted through the ExD cell into the HCD cell in the absence of electrons, where ECD was occurring. A set of seven voltage parameters of the ExD cell controlling the emitting and confinement of electrons were optimized to ensure efficient electron capture by the protein ions in the HCD cell (Table S1). Post-ECD collisional activation was applied by setting CE values between 150V and 200V to minimize the effect of electron capture without dissociation (ECnoD).[57] All HCD and ECD MS/MS spectra were collected with the noise threshold set at 3, a resolution of 200000 at *m/z* 400, AGC target of 1e6, and maximum inject time of 200 ms. Between 100 and 200 scans were averaged for each spectrum.

Data Analysis.

Data Processing and Fragment Assignment.—Raw MS/MS spectra were deconvoluted using Thermo BioPharma Finder 5.0 (Xtract algorithm) and deconvoluted mass lists were exported as .csv files for fragment assignment in ClipsMS.[61] The mass tolerance was set at 3 ppm and the smallest internal fragment size was set at 5 amino acids. For sequence coverage analysis of NIST mAb, modifications relating to disulfide bond cleavages and hydrogen gains expected for ECD were considered. Similarly, for disulfide connectivity analysis of NIST mAb, modifications applying one hydrogen loss on each cysteine forming intra-chain disulfide bonds to suggest the integrity of the disulfide bond were included. For drug conjugation sites analysis of ADC, modifications considering one or two intact DM1 conjugation were searched for, depending on the identity of the isolated precursor ion (DAR 1 or DAR 2 ions). Water and ammonia losses were considered for HCD fragmentation, and glycosylations including G0F, G1F, and G2F were considered for heavy chain fragments. Four terminal fragment types including *b, c, y, z* were searched for ECD, while only *b* and *y* terminal fragments were searched for HCD. As for internal fragment matching, only *by* internal fragments were searched for HCD and *cz* internal fragments for ECD. All terminal fragments were assigned before considering internal fragments, and all overlapping internal fragments due to the arrangement and/or frameshift ambiguity[64] were removed. The fragment search was done separately for light chain and heavy chain for a single TD-MS dataset, *i.e.*, one TD-MS spectrum was searched once against the light chain sequence and once against the heavy chain sequence. For overlapping assignments shared by the light chain and heavy chain, two factors were considered to remove these duplicates: 1). If a deconvoluted mass is assigned as a terminal fragment for one chain while as an internal fragment for the other chain (both within 3 ppm), the terminal fragment assignment was retained; 2). If a deconvoluted mass is assigned as an internal fragment for either chain, the one with the lower ppm error was retained. After fragment matching and duplicates removal, all assigned internal fragments were further refined by a two-step manual validation process: 1). Examine the isotopic profile of every assigned internal fragment to eliminate poorly fitted uncertain assignments; 2). Compare the assignment results with the theoretical fragment lists generated by ProteinProspector v 6.4.2[73] to eliminate any possible overlap between assigned internal fragments and theoretical terminal fragments together with their possible modifications such as neutral losses. The assignment results for every isolated charge state of NIST mAb were combined, as well for every isolated ion of ADC after manual validation.

Protein Sequence Coverage.—Protein sequence coverage is calculated by the number of observed inter-residue cleavage sites divided by the total number of possible inter-residue cleavage sites on the protein backbone.

S-S connectivity mismatch rate.—S-S connectivity mismatch rate is calculated by dividing the number of fragments that cause mismatched S-S connectivity (orange-colored fragments in Figure 4 and S3) by the total number of fragments that can determine S-S connectivity (green-colored fragments in Figure 4 and S3) and fragments that cause mismatched S-S connectivity.

RESULTS AND DISCUSSION

Internal fragments increase the sequence coverage of intact mAbs.

Native MS provides a global overview of the composition of intact mAbs, including major glycoforms (Figure 1A and B); however, their characterization requires comprehensive sequence analysis. Assigning internal fragments can significantly enhance the sequence information obtained from intact mAbs. To demonstrate this, two fragmentation methods, ECD and HCD, were applied on the five most abundant charge states of intact NIST mAb (22+ to 26+). An example ECD spectrum of intact NIST mAb is shown in Figure S2. ECD of $[NIST + 25H]^{25+}$ precursor ion generated many informative product ions along with charge reduced precursor ions (Figure S2A and B). Terminal and internal fragments from both heavy and light chains are observed, demonstrating that more information can be obtained by assigning these previously ignored signals (Figure S2B). Importantly, internal fragments provide complementary sequence information to terminal fragments, spanning most of the interior sequence of both chains that cannot be reached by terminal fragments (Figure S2C and D).

The major obstacle that prevents comprehensive sequence coverage of intact mAbs is the presence of numerous disulfide bonds that contribute to maintaining protein structure and stability. For terminal fragments to cover the disulfide bonded sequence region, cleavages of both protein backbone and disulfide bonds are required. However, internal fragments can access these highly constrained regions without the need of breaking disulfide bonds, thus having the potential to substantially enhance sequence information of intact mAbs.[67] Additionally, internal fragments contain two cleavage sites while terminal fragments only contain one, making internal fragments naturally more information-rich than terminal fragments. This also leads to an increase in the sequence coverage obtained when considering internal fragments. To investigate the additional sequence information that can be obtained by assigning internal fragments, we combined the ECD and HCD TD-MS results from each isolated charge state of intact NIST mAb. Inclusion of internal fragments increases the sequence coverage of the light chain from 54% to 83% and the heavy chain from 28% to 72%, which combined to an increase from 36% to 76% for the whole NIST mAb (Figure 2), which to our knowledge is the highest sequence coverage of an intact mAb achieved by TD-MS. A more significant increase is observed for heavy chain (44%) than light chain (29%), demonstrating that assigning internal fragments becomes more valuable with increasing protein size.

As expected, the significant increase in sequence coverage is largely due to improved access by internal fragments of the highly disulfide constrained regions, which cannot be reached by terminal fragments (Figure 2 and Table S2). For example, the disulfide constrained sequence between Cys133 to Cys193 of the light chain is almost exclusively accessed by internal fragments (Figure 3A). The same is true for sequence regions Cys147-Cys203 and Cys264-Cys324 of the heavy chain (Figure 3B). For the intact NIST mAb, assigning internal fragments increases the coverage of the non-disulfide constrained sequence by 34%, compared to a more significant increase of 44% in the disulfide constrained sequence.

The sequence of complementarity determining regions (CDRs) need to be unambiguously determined, as it is responsible of antigen target specificity of mAbs. Additionally, chemical liabilities such as deamidation, isomerization, and oxidation in CDRs are problematic; therefore, they need to be fully characterized.[75] In total, an increase from 53% to 60% of amino acids in CDR are confirmed after assigning internal fragments, demonstrating that more insight of this critical region can be gleaned with the inclusion of internal fragments. Despite the improvement, the sequence coverage of CDRs is still far from optimal, particularly for the longer heavy chain (70% for light chain vs. 51% for heavy chain). Therefore, complementary techniques such as middle-down and bottom-up approaches, are needed to unambiguously determine the CDRs sequence, and internal fragments can play a pivotal role in these techniques.

Internal fragments can identify mAb PTMs, including intra-chain S-S connectivity and N-glycosylations.

Previously, our group demonstrated that internal fragments that retain intact disulfide bonds can be used to determine S-S connectivity of intact proteins (Figure S3).[67] This encourages us to explore the utility of such fragments to determine intra-chain S-S connectivity of intact NIST mAb, which is comprised of 16 disulfide bonds. HCD is known to only cleave the protein backbone while maintaining the integrity of disulfide bonds; therefore, we applied HCD on intact NIST mAb to generate such fragments to determine S-S connectivity.

A hydrogen loss was applied on every cysteine forming intra-chain disulfide bonds to indicate their integrity after HCD fragmentation, and fragments that traverse an intact disulfide bond can determine S-S connectivity (green fragments in Figure 4 and S3). For example, for the light chain, 52 terminal fragments and 12 internal fragments traverse S-S bond I, 17 terminal fragments traverse S-S bond II, and 6 terminal fragments traverse both disulfide bonds, clearly demonstrating the S-S bonding pattern of these two disulfide bonds (Figure 4A). The value of analyzing internal fragments to determine intra-chain S-S connectivity is exhibited more clearly in the case of the heavy chain. The two disulfide bonds close to either terminus of the heavy chain, S-S bond I and S-S bond IV, are traversed by 89 terminal fragments and 9 internal fragments. However, the two middle disulfide bonds, S-S bond II and S-S bond III, are only traversed by 24 internal fragments but no terminal fragments (Figure 4B). Fragments traversing two intact disulfide bonds were also observed. For example, S-S bond I and II are traversed by 10 terminal fragments and 1 internal fragment, and S-S bond III and IV are traversed by 3 terminal fragments and 9 internal fragments. In contrast, no terminal fragments but 2 internal fragments traverse S-S bond II and III, the middle two disulfide bonds. This corroborates the ability of internal fragments to access the interior regions of the protein sequence and disulfide bonds, particularly for larger proteins. These results demonstrate the intra-chain S-S connectivity of the NIST mAb heavy chain, and importantly, the two middle S-S bonding patterns can only be determined by internal fragments.

Although much rarer, HCD can cleave both the protein backbone and disulfide bonds simultaneously, generating two types of fragments that have differing ramifications in the determination of S-S connectivity. These fragments are represented as blue and orange

fragments in Figure 4 and Figure S3. The blue fragments either do not bridge any dehydrocysteines, or they traverse though intact disulfide bonds and from inside a disulfide bond simultaneously. These fragments do not directly contribute to the determination of S-S connectivity. The orange fragments, on the other hand, do not traverse through existing disulfide bonds, but rather they only cross through non-connected dehydrocysteines from inside a disulfide bond, thus lead to mismatched S-S connectivity. For example, one such fragment was observed for the light chain (Figure 4A, Table S2) and six fragments for the heavy chain (Figure 4B and C, Table S3), resulting in S-S connectivity mismatch rates of 1.1% for the light chain and 3.9% for the heavy chain. The low mismatch rates support the concept of using fragments retaining intact disulfide bonds to determine intra-chain S-S connectivity of intact mAbs. Alternatively, a small portion of disulfide bonds of NIST mAb ions may have been present in reduced form prior to HCD fragmentation due to high source temperature and high in-source energy, leading to disulfide scrambling. This could also result in the formation of “S-S mismatched fragments” (orange fragments in Figure 4 and Figure S3). However, it is difficult to distinguish between these two possibilities by HCD TD-MS alone. A study comparing the HCD fragmentation pattern of mAbs in both native and heat-stressed conditions could shed light on the contribution of disulfide scrambling.

In addition to determining intra-chain S-S connectivity, assigning internal fragments also contributes to identifying N-glycosylations, a ubiquitous PTM class of mAbs. After combining data from five isolated precursor charge states, ECD and HCD TD-MS of intact NIST mAb generates only 9 unique C-terminal fragments containing N-glycosylations, with 2 containing G0F, 5 containing G1F, and 2 containing G2F (Figure S4). However, when internal fragments were considered, an additional 25 fragments containing G0F, 42 fragments containing G1F, and 34 fragments containing G2F were assigned, demonstrating the power of analyzing internal fragments for N-glycosylation identification (Figure S4). This is mainly attributed to the ability of internal fragments to access interior protein sequence constrained by disulfide bonds that are typically inaccessible to terminal fragments. The inclusion of internal fragments can potentially also contribute to identifying other common PTMs of mAbs such as oxidation and deamidation, improving the accuracy and consistency of mAb production.

Internal fragments can determine drug conjugation sites of lysine-linked ADCs.

The promising results obtained from TD-MS of intact NIST mAb inspired us to push one step further to explore the utility of internal fragments for the determination of drug conjugation sites of ADCs, an even more heterogeneous drug class. To achieve this, we took a similar TD-MS approach by applying both ECD and HCD on a previously well chracterized non specific lysine-linked ADC.[12]

Native MS reveals the maytansinoid DM1 distribution profile of the intact ADC. Seven major DAR species were observed (DAR0-DAR7), confirming the highly heterogeneous nature of this ADC (Figure 1C and D). DAR 1 and DAR 2 species of the major four charge states (22+ to 25+) were isolated and fragmented with ECD and HCD (see Experimental Section). Similar to the NIST mAb, ECD fragmentation of the intact ADC generated both terminal and internal fragments from both chains of the anibody (Figure S5). Importantly,

DM1-bound fragments were also observed, providing direct evidence to determine drug conjugation sites (Figure S5 and S6). The inherently random lysine conjugation makes the determination of drug conjugation sites of lysine-linked ADC challenging. For example, a total of 90 potential conjugation sites exist on the ADC used in this study after excluding the clipped C-terminal lysine on the heavy chain, including 11 from light chain and 34 from heavy chain. Nervertheless, applying two fragmentation methods, ECD and HCD, on the intact ADC allowed us to unambigously determine a large fraction of potential conjugation sites, in which internal fragments played a critical role.

Here, we define *localizing a conjugation site* as when the conjugation can be specified on an exact lysine resiue, while *identifying a conjugation site* is defined as when the conjugation can only be confirmed on several possible lysine residues. TD-MS of the ADC generated only 8 DM1-bound terminal fragments on the light chain, includng 5 one-DM1-bound, and 3 two-DM1-bound fragments (Figure 5A). The two-DM1-bound terminal fragment c_{85} conclusively localized the conjugation sites to K46 and K67, whereas all other assigned terminal fragments could not localize any additional conjugation sites, but only identify 2 other conjugation sites on the light chain. Unsurprisingly, assigning internal fragments significantly improved the determination of DM1 conjugation sites. TD-MS of the ADC generated 61 one-DM1-bound and 15 two-DM1-bound internal fragments on the light chain, which localized 3 more conjugation sites (K106, K114, K133) and narrowed down the identified two conjugation sites to 4 lysine residues (K153, K160, K170, K175) (Figure 5A). For example, the assignment of one-DM1-bound internal fragments $cz_{96–113}$, $cz_{97–113}$, $cz_{98–111}$, and $by_{104–112}$ localized the conjugation site to K106, $cz_{112–125}$ and $cz_{114–124}$ localized the conjugation site to K114, $cz_{119–152}$, $cz_{128–140}$, and $by_{133–141}$ localized the conjugation site to K133 (Figure 5A). Similar results were observed for the heavy chain. TD-MS of the ADC generated only 11 DM1-bound terminal fragments (6 one-DM1-bound and 5 two-DM1-bound) but 167 DM1-bound internal fragments (107 one-DM1-bound and 60 two-DM1-bound) on the heavy chain. With terminal fragments alone, no conjugation sites could be localized, but 4 were identified; however, after considering internal fragments, 9 conjugations sites were localized (K13, K43, K89, K127, K139, K153, K252, K254, K323), and 10 additional conjugations sites were identified. In summary, for the intact ADC, only 16 conjugation sites were confirmed (4 localized and 12 identified) with terminal fragments alone, whereas this number was increased to 52 (28 localized, 24 identified) upon inclusion of internal fragments, covering approximately 58% of all putative conjugation sites of the antibody (Table S3). Although lower than the previously reported 83% coverage achieved by peptide mapping,[12] this result still demonstrates the value of analyzing TD-MS internal fragments to determine drug conjugation sites of ADCs.

CONCLUSIONS

Here we report for the first time the benefits of analyzing internal fragments in the TD-MS characterization of intact NIST mAb and a heterogeneous lysine-linked ADC. Inclusion of internal fragments significantly increases the sequence coverage of intact mAbs to over 75% by accessing the disulfide constrained regions that are hardly accessed by terminal fragments, particularly for the larger heavy chain. Important PTM information, including disulfide linkage patterns and N-glycosylations, can be obtained by including internal

fragments. Internal fragments retaining intact disulfide bonds were used to determine the intra-chain S-S connectivity of an intact mAb, an important CQA required for accurate determination during antibody production. And importantly, we show that internal fragments can help pinpoint drug conjugation sites of highly heterogeneous lysine-linked ADCs, an attribute that is as important as, but not as well evaluated as characteristics like DAR and drug distribution.

It should be noted that limitations still exist for TD-MS of mAbs despite the added benefit of assigning internal fragments. For example, only ~60% sequence coverage on the CDRs of intact mAbs and ~58% drug conjugation site coverage of intact lysine-linked ADCs were achieved, which do not meet the requirement of biologics development in the pharmaceutical industry. Identifying uncommon, low intensity glycoforms also remains challenging. Furthermore, the heavy reliance on manual inspection during data analysis likely prevents the widespread adoption of this approach. Therefore, complementary techniques such as middle-down MS and bottom-up MS approaches are currently still required to achieve more comprehensive and efficient therapeutics characterization. For instance, denatured reversed-phase LC-MS of intact and FabRICATOR/reduced treated mAbs result in smaller protein subunits with higher charge states, thus enabling more efficient MS/MS fragmentation. Nevertheless, the results presented here demonstrate the multiple benefits of assigning internal fragments to obtain critical structural information of intact mAbs and ADCs.

From an analytical viewpoint, the raw data for internal fragments is present in the TD mass spectra, but assigning the peaks in the spectra to uncover this *hidden treasure* can be a fruitful endeavor, especially for characterizing therapeutic proteins. Although bottom-up MS is firmly entrenched in pharmaceutical industry workflows, TD-MS offers potential benefits if robust automation and computational support can be established. Once this native TD-MS method has fully evolved and matured to a point where it is comparable to the already-established bottom-up approaches, one can realize the significantly reduced amount of sample handling (no denaturation, reduction or alkylation); therefore, there is less opportunity to introduce sample handling-related artifacts. This study should also suggest that the incorporation of internal fragments can be applied to bottom-up and middle-down MS analysis of mAbs and ADCs, potentially extending their characterization to a near complete level on a routine basis.

Supplementary Material

Refer to Web version on PubMed Central for supplementary material.

ACKNOWLEDGMENT

J.A.L. and R.R.O.L. acknowledge support from the US National Institutes of Health (R01GM103479, R35GM145286) and the US Department of Energy (DE-FC02-02ER63421). C.L. acknowledges support from the Ruth L. Kirschstein National Research Service Award program (GM007185).

References

1. Kisalu NK; Idris AH; Weidle C; Flores-Garcia Y; Flynn BJ; Sack BK; Murphy S; Schön A; Freire E; Francica JR; Miller AB; Gregory J; March S; Liao H-X; Haynes BF; Wiehe K; Trama AM; Saunders KO; Gladden MA; Monroe A; Bonsignori M; Kanekiyo M; Wheatley AK; McDermott AB; Farney SK; Chuang G-Y; Zhang B; Kc N; Chakravarty S; Kwong PD; Sinnis P; Bhatia SN; Kappe SHI; Sim BKL; Hoffman SL; Zavala F; Pancera M; Seder RA, A human monoclonal antibody prevents malaria infection by targeting a new site of vulnerability on the parasite. Nature Medicine 2018, 24 (4), 408–416.
2. London M; Gallo E, Epidermal growth factor receptor (EGFR) involvement in epithelial-derived cancers and its current antibody-based immunotherapies. Cell Biology International 2020, 44 (6), 1267–1282. [PubMed: 32162758]
3. Schrama D; Reisfeld RA; Becker JC, Antibody targeted drugs as cancer therapeutics. Nature Reviews Drug Discovery 2006, 5 (2), 147–159. [PubMed: 16424916]
4. Bebbington C; Yarranton G, Antibodies for the treatment of bacterial infections: current experience and future prospects. Current Opinion in Biotechnology 2008, 19 (6), 613–619. [PubMed: 19000762]
5. Beck A; Wurch T; Bailly C; Corvaia N, Strategies and challenges for the next generation of therapeutic antibodies. Nature Reviews Immunology 2010, 10 (5), 345–352.
6. Mould DR; Meibohm B, Drug Development of Therapeutic Monoclonal Antibodies. BioDrugs 2016, 30 (4), 275–293. [PubMed: 27342605]
7. Marston HD; Paules CI; Fauci AS, Monoclonal Antibodies for Emerging Infectious Diseases — Borrowing from History. New England Journal of Medicine 2018, 378 (16), 1469–1472. [PubMed: 29513615]
8. Frenzel A; Hust M; Schirrmann T, Expression of recombinant antibodies. Front Immunol 2013, 4, 217. [PubMed: 23908655]
9. Sissolak B; Lingg N; Sommeregger W; Striedner G; Vorauer-Uhl K, Impact of mammalian cell culture conditions on monoclonal antibody charge heterogeneity: an accessory monitoring tool for process development. Journal of Industrial Microbiology and Biotechnology 2019, 46 (8), 1167–1178. [PubMed: 31175523]
10. Rathore AS; Winkle H, Quality by design for biopharmaceuticals. Nature Biotechnology 2009, 27 (1), 26–34.
11. Meibohm B, Pharmacokinetics and Pharmacodynamics of Therapeutic Peptides and Proteins. In Pharmaceutical Biotechnology: Fundamentals and Applications, Crommelin DJA; Sindelar RD; Meibohm B, Eds. Springer International Publishing: Cham, 2019; pp 105–137.
12. Luo Q; Chung HH; Borths C; Janson M; Wen J; Joubert MK; Wypych J, Structural Characterization of a Monoclonal Antibody–Maytansinoid Immunoconjugate. Analytical Chemistry 2016, 88 (1), 695–702. [PubMed: 26629796]
13. Chari RVJ; Miller ML; Widdison WC, Antibody–Drug Conjugates: An Emerging Concept in Cancer Therapy. Angewandte Chemie International Edition 2014, 53 (15), 3796–3827. [PubMed: 24677743]
14. Peters C; Brown S, Antibody–drug conjugates as novel anti-cancer chemotherapeutics. Bioscience Reports 2015, 35 (4), e00225. [PubMed: 26182432]
15. Khongorzul P; Ling CJ; Khan FU; Ihsan AU; Zhang J, Antibody–Drug Conjugates: A Comprehensive Review. Molecular Cancer Research 2020, 18 (1), 3–19. [PubMed: 31659006]
16. Abdollahpour-Alitappeh M; Lotfinia M; Gharibi T; Mardaneh J; Farhadihosseinabadi B; Larki P; Faghfourian B; Sepehr KS; Abbaszadeh-Goudarzi K; Abbaszadeh-Goudarzi G; Johari B; Zali MR; Bagheri N, Antibody–drug conjugates (ADCs) for cancer therapy: Strategies, challenges, and successes. Journal of Cellular Physiology 2019, 234 (5), 5628–5642. [PubMed: 30478951]
17. Sang H; Lu G; Liu Y; Hu Q; Xing W; Cui D; Zhou F; Zhang J; Hao H; Wang G; Ye H, Conjugation site analysis of antibody-drug-conjugates (ADCs) by signature ion fingerprinting and normalized area quantitation approach using nano-liquid chromatography coupled to high resolution mass spectrometry. Analytica Chimica Acta 2017, 955, 67–78. [PubMed: 28088282]

18. Ricart AD, Antibody-Drug Conjugates of Calicheamicin Derivative: Gemtuzumab Ozogamicin and Inotuzumab Ozogamicin. Clinical Cancer Research 2011, 17 (20), 6417–6427. [PubMed: 22003069]
19. Lambert JM; Chari RVJ, Ado-trastuzumab Emtansine (T-DM1): An Antibody–Drug Conjugate (ADC) for HER2-Positive Breast Cancer. Journal of Medicinal Chemistry 2014, 57 (16), 6949–6964. [PubMed: 24967516]
20. Yoder NC; Bai C; Tavares D; Widdison WC; Whiteman KR; Wilhelm A; Wilhelm SD; Mcshea MA; Maloney EK; Ab O; Wang L; Jin S; Erickson HK; Keating TA; Lambert JM, A Case Study Comparing Heterogeneous Lysine- and Site-Specific Cysteine-Conjugated Maytansinoid Antibody-Drug Conjugates (ADCs) Illustrates the Benefits of Lysine Conjugation. Molecular Pharmaceutics 2019, 16 (9), 3926–3937. [PubMed: 31287952]
21. Haque M; Forte N; Baker JR, Site-selective lysine conjugation methods and applications towards antibody–drug conjugates. Chemical Communications 2021, 57 (82), 10689–10702. [PubMed: 34570125]
22. Huang Y; Mou S; Wang Y; Mu R; Liang M; Rosenbaum AI, Characterization of Antibody–Drug Conjugate Pharmacokinetics and in Vivo Biotransformation Using Quantitative Intact LC-HRMS and Surrogate Analyte LC-MRM. Analytical Chemistry 2021, 93 (15), 6135–6144. [PubMed: 33835773]
23. Zhu X; Huo S; Xue C; An B; Qu J, Current LC-MS-based strategies for characterization and quantification of antibody-drug conjugates. Journal of Pharmaceutical Analysis 2020, 10 (3), 209–220. [PubMed: 32612867]
24. Bobály B; Fleury-Souverain S; Beck A; Veuthey J-L; Guillarme D; Fekete S, Current possibilities of liquid chromatography for the characterization of antibody-drug conjugates. Journal of Pharmaceutical and Biomedical Analysis 2018, 147, 493–505. [PubMed: 28688616]
25. Agarwal P; Bertozzi CR, Site-Specific Antibody–Drug Conjugates: The Nexus of Bioorthogonal Chemistry, Protein Engineering, and Drug Development. Bioconjugate Chemistry 2015, 26 (2), 176–192. [PubMed: 25494884]
26. Shen B-Q; Xu K; Liu L; Raab H; Bhakta S; Kenrick M; Parsons-Reponte KL; Tien J; Yu S-F; Mai E; Li D; Tibbitts J; Baudys J; Saad OM; Scales SJ; McDonald PJ; Hass PE; Eigenbrot C; Nguyen T; Solis WA; Fuji RN; Flagella KM; Patel D; Spencer SD; Khawli LA; Ebens A; Wong WL; Vandlen R; Kaur S; Sliwkowski MX; Scheller RH; Polakis P; Junutula JR, Conjugation site modulates the in vivo stability and therapeutic activity of antibody-drug conjugates. Nature Biotechnology 2012, 30 (2), 184–189.
27. Wakankar A; Chen Y; Gokarn Y; Jacobson FS, Analytical methods for physicochemical characterization of antibody drug conjugates. mAbs 2011, 3 (2), 161–172. [PubMed: 21441786]
28. Huang RYC; Chen G, Characterization of antibody–drug conjugates by mass spectrometry: advances and future trends. Drug Discovery Today 2016, 21 (5), 850–855. [PubMed: 27080148]
29. Campuzano IDG; Netirojjanakul C; Nshanian M; Lippens JL; Kilgour DPA; Van Orden S; Loo JA, Native-MS Analysis of Monoclonal Antibody Conjugates by Fourier Transform Ion Cyclotron Resonance Mass Spectrometry. Analytical Chemistry 2018, 90 (1), 745–251. [PubMed: 29193956]
30. Campuzano IDG; Nshanian M; Spahr C; Lantz C; Netirojjanakul C; Li H; Wongkongkathep P; Wolff JJ; Loo JA, High Mass Analysis with a Fourier Transform Ion Cyclotron Resonance Mass Spectrometer: From Inorganic Salt Clusters to Antibody Conjugates and Beyond. Journal of the American Society for Mass Spectrometry 2020, 31 (5), 1155–1162. [PubMed: 32196330]
31. Junutula JR; Raab H; Clark S; Bhakta S; Leipold DD; Weir S; Chen Y; Simpson M; Tsai SP; Dennis MS; Lu Y; Meng YG; Ng C; Yang J; Lee CC; Duenas E; Gorrell J; Katta V; Kim A; McDorman K; Flagella K; Venook R; Ross S; Spencer SD; Lee Wong W; Lowman HB; Vandlen R; Sliwkowski MX; Scheller RH; Polakis P; Mallet W, Site-specific conjugation of a cytotoxic drug to an antibody improves the therapeutic index. Nature Biotechnology 2008, 26 (8), 925–932.
32. Song Y; Gao J; Meng Q; Tang F; Wang Y; Zeng Y; Huang W; Shao H; Zhou H, Conjugation site characterization of antibody–drug conjugates using electron-transfer/higher-energy collision dissociation (EThcD). Analytica Chimica Acta 2023, 340978. [PubMed: 36925279]
33. Afar DEH; Bhaskar V; Ibsen E; Breinberg D; Henshall SM; Kench JG; Drobnjak M; Powers R; Wong M; Evangelista F; O'Hara C; Powers D; DuBridge RB; Caras I; Winter R; Anderson T; Solvason N; Stricker PD; Cordon-Cardo C; Scher HI; Grygiel JJ; Sutherland RL; Murray

R; Ramakrishnan V; Law DA, Preclinical validation of anti-TMEFF2-auristatin E–conjugated antibodies in the treatment of prostate cancer. Molecular Cancer Therapeutics 2004, 3 (8), 921–932. [PubMed: 15299075]

34. Bongers J; Cummings JJ; Ebert MB; Federici MM; Gledhill L; Gulati D; Hilliard GM; Jones BH; Lee KR; Mozdzanowski J; Naimoli M; Burman S, Validation of a peptide mapping method for a therapeutic monoclonal antibody: what could we possibly learn about a method we have run 100 times? Journal of Pharmaceutical and Biomedical Analysis 2000, 21 (6), 1099–1128. [PubMed: 10708395]
35. Fleming MS; Zhang W; Lambert JM; Amphlett G, A reversed-phase high-performance liquid chromatography method for analysis of monoclonal antibody–maytansinoid immunoconjugates. Analytical Biochemistry 2005, 340 (2), 272–278. [PubMed: 15840500]
36. Ayoub D; Bertaccini D; Diemer H; Wagner-Rousset E; Colas O; Cianférani S; Van Dorsselaer A; Beck A; Schaeffer-Reiss C, Characterization of the N-Terminal Heterogeneities of Monoclonal Antibodies Using In-Gel Charge Derivatization of α-Amines and LC-MS/MS. Analytical Chemistry 2015, 87 (7), 3784–3790. [PubMed: 25769014]
37. Wang L; Amphlett G; Blättler WA; Lambert JM; Zhang W, Structural characterization of the maytansinoid–monoclonal antibody immunoconjugate, huN901–DM1, by mass spectrometry. Protein Science 2005, 14 (9), 2436–2446. [PubMed: 16081651]
38. Janin-Bussat M-C; Dillenbourg M; Corvaia N; Beck A; Klinguer-Hamour C, Characterization of antibody drug conjugate positional isomers at cysteine residues by peptide mapping LC–MS analysis. Journal of Chromatography B 2015, 981–982, 9–13.
39. Said N; Gahoual R; Kuhn L; Beck A; François Y-N; Leize-Wagner E, Structural characterization of antibody drug conjugate by a combination of intact, middle-up and bottom-up techniques using sheathless capillary electrophoresis – Tandem mass spectrometry as nanoESI infusion platform and separation method. Analytica Chimica Acta 2016, 918, 50–59. [PubMed: 27046210]
40. Song Y; Schowen RL; Borchardt RT; Topp EM, Effect of 'pH' on the rate of asparagine deamidation in polymeric formulations: 'pH'–rate profile. Journal of Pharmaceutical Sciences 2001, 90 (2), 141–156. [PubMed: 11169531]
41. Nielsen ML; Vermeulen M; Bonaldi T; Cox J; Moroder L; Mann M, Iodoacetamide-induced artifact mimics ubiquitination in mass spectrometry. Nature Methods 2008, 5 (6), 459–460. [PubMed: 18511913]
42. Lippincott J; Apostol I, Carbamylation of Cysteine: A Potential Artifact in Peptide Mapping of Hemoglobins in the Presence of Urea. Analytical Biochemistry 1999, 267 (1), 57–64. [PubMed: 9918655]
43. Fornelli L; Srzentić K; Huguet R; Mullen C; Sharma S; Zabrouskov V; Fellers RT; Durbin KR; Compton PD; Kelleher NL, Accurate Sequence Analysis of a Monoclonal Antibody by Top-Down and Middle-Down Orbitrap Mass Spectrometry Applying Multiple Ion Activation Techniques. Analytical Chemistry 2018, 90 (14), 8421–8429. [PubMed: 29894161]
44. Srzentić K; Nagornov KO; Fornelli L; Lobas AA; Ayoub D; Kozhinov AN; Gasilova N; Menin L; Beck A; Gorshkov MV; Aizikov K; Tsybin YO, Multiplexed Middle-Down Mass Spectrometry as a Method for Revealing Light and Heavy Chain Connectivity in a Monoclonal Antibody. Analytical Chemistry 2018, 90 (21), 12527–12535. [PubMed: 30252447]
45. Fornelli L; Ayoub D; Aizikov K; Beck A; Tsybin YO, Middle-Down Analysis of Monoclonal Antibodies with Electron Transfer Dissociation Orbitrap Fourier Transform Mass Spectrometry. Analytical Chemistry 2014, 86 (6), 3005–3012. [PubMed: 24588056]
46. Cejkov M; Greer T; Johnson ROB; Zheng X; Li N, Electron Transfer Dissociation Parameter Optimization Using Design of Experiments Increases Sequence Coverage of Monoclonal Antibodies. Journal of the American Society for Mass Spectrometry 2021, 32 (3), 762–771. [PubMed: 33596068]
47. Chen B; Lin Z; Zhu Y; Jin Y; Larson E; Xu Q; Fu C; Zhang Z; Zhang Q; Pritts WA; Ge Y, Middle-Down Multi-Attribute Analysis of Antibody-Drug Conjugates with Electron Transfer Dissociation. Analytical Chemistry 2019, 91 (18), 11661–11669. [PubMed: 31442030]
48. Hernandez-Alba O; Houel S; Hessmann S; Erb S; Rabuka D; Huguet R; Josephs J; Beck A; Drake PM; Cianférani S, A Case Study to Identify the Drug Conjugation Site of a Site-Specific

Antibody-Drug-Conjugate Using Middle-Down Mass Spectrometry. Journal of the American Society for Mass Spectrometry 2019, 30 (11), 2419–2429. [PubMed: 31429052]

49. Larson EJ; Zhu Y; Wu Z; Chen B; Zhang Z; Zhou S; Han L; Zhang Q; Ge Y, Rapid Analysis of Reduced Antibody Drug Conjugate by Online LC-MS/MS with Fourier Transform Ion Cyclotron Resonance Mass Spectrometry. Analytical Chemistry 2020, 92 (22), 15096–15103. [PubMed: 33108180]
50. Watts E; Williams JD; Miesbauer LJ; Bruncko M; Brodbelt JS, Comprehensive Middle-Down Mass Spectrometry Characterization of an Antibody–Drug Conjugate by Combined Ion Activation Methods. Analytical Chemistry 2020, 92 (14), 9790–9798. [PubMed: 32567851]
51. Fornelli L; Damoc E; Thomas PM; Kelleher NL; Aizikov K; Denisov E; Makarov A; Tsybin YO, Analysis of Intact Monoclonal Antibody IgG1 by Electron Transfer Dissociation Orbitrap FTMS. Molecular & Cellular Proteomics 2012, 11 (12), 1758–1767. [PubMed: 22964222]
52. Mao Y; Valeja SG; Rouse JC; Hendrickson CL; Marshall AG, Top-Down Structural Analysis of an Intact Monoclonal Antibody by Electron Capture Dissociation-Fourier Transform Ion Cyclotron Resonance-Mass Spectrometry. Analytical Chemistry 2013, 85 (9), 4239–4246. [PubMed: 23551206]
53. Jin Y; Lin Z; Xu Q; Fu C; Zhang Z; Zhang Q; Pritts WA; Ge Y, Comprehensive characterization of monoclonal antibody by Fourier transform ion cyclotron resonance mass spectrometry. mAbs 2019, 11 (1), 106–115. [PubMed: 30230956]
54. Lodge JM; Schauer KL; Brademan DR; Riley NM; Shishkova E; Westphall MS; Coon JJ, Top-Down Characterization of an Intact Monoclonal Antibody Using Activated Ion Electron Transfer Dissociation. Analytical Chemistry 2020, 92 (15), 10246–10251. [PubMed: 32608969]
55. Shaw JB; Liu W; Vasil Ev YV; Bracken CC; Malhan N; Guthals A; Beckman JS; Voinov VG, Direct Determination of Antibody Chain Pairing by Top-down and Middle-down Mass Spectrometry Using Electron Capture Dissociation and Ultraviolet Photodissociation. Anal. Chem 2020, 92 (1), 766–773. [PubMed: 31769659]
56. Srzentić K; Fornelli L; Tsybin YO; Loo JA; Seckler H; Agar JN; Anderson LC; Bai DL; Beck A; Brodbelt JS; Van Der Burgt YEM; Chamot-Rooke J; Chatterjee S; Chen Y; Clarke DJ; Danis PO; Diedrich JK; D'Ippolito RA; Dupré M; Gasilova N; Ge Y; Goo YA; Goodlett DR; Greer S; Haselmann KF; He L; Hendrickson CL; Hinkle JD; Holt MV; Hughes S; Hunt DF; Kelleher NL; Kozhinov AN; Lin Z; Malosse C; Marshall AG; Menin L; Millikin RJ; Nagornov KO; Nicolardi S; Paša-Tolić L; Pengelley S; Quebbemann NR; Resemann A; Sandoval W; Sarin R; Schmitt ND; Shabanowitz J; Shaw JB; Shortreed MR; Smith LM; Sobott F; Suckau D; Toby T; Weisbrod CR; Wildburger NC; Yates JR; Yoon SH; Young NL; Zhou M, Interlaboratory Study for Characterizing Monoclonal Antibodies by Top-Down and Middle-Down Mass Spectrometry. Journal of the American Society for Mass Spectrometry 2020, 31 (9), 1783–1802. [PubMed: 32812765]
57. Fornelli L; Ayoub D; Aizikov K; Liu X; Damoc E; Pevzner PA; Makarov A; Beck A; Tsybin YO, Top-down analysis of immunoglobulin G isotypes 1 and 2 with electron transfer dissociation on a high-field Orbitrap mass spectrometer. Journal of Proteomics 2017, 159, 67–76. [PubMed: 28242452]
58. Fekete S; Guillarme D; Sandra P; Sandra K, Chromatographic, Electrophoretic, and Mass Spectrometric Methods for the Analytical Characterization of Protein Biopharmaceuticals. Analytical Chemistry 2016, 88 (1), 480–507. [PubMed: 26629607]
59. Larson EJ; Roberts DS; Melby JA; Buck KM; Zhu Y; Zhou S; Han L; Zhang Q; Ge Y, High-Throughput Multi-attribute Analysis of Antibody-Drug Conjugates Enabled by Trapped Ion Mobility Spectrometry and Top-Down Mass Spectrometry. Analytical Chemistry 2021, 93 (29), 10013–10021. [PubMed: 34258999]
60. Davis TK; Jennings ME, Site-Specific Conjugation Quantitation of a Cysteine-Conjugated Antibody–Drug Conjugate Using Stable Isotope Labeling Peptide Mapping LC–MS/MS Analysis. Analytical Chemistry 2022, 94 (6), 2772–2778. [PubMed: 35100801]
61. Lantz C; Zenaidee MA; Wei B; Hemminger Z; Ogorzalek Loo RR; Loo JA, ClipsMS: An Algorithm for Analyzing Internal Fragments Resulting from Top-Down Mass Spectrometry. J. Proteome Res 2021, 20 (4), 1928–1935. [PubMed: 33650866]

62. Durbin KR; Skinner OS; Fellers RT; Kelleher NL, Analyzing internal fragmentation of electrosprayed ubiquitin ions during beam-type collisional dissociation. J. Am. Soc. Mass Spectrom 2015, 26 (5), 782–787. [PubMed: 25716753]

63. Zenaidee MA; Lantz C; Perkins T; Jung W; Loo RRO; Loo JA, Internal Fragments Generated by Electron Ionization Dissociation Enhance Protein Top-Down Mass Spectrometry. J. Am. Soc. Mass Spectrom 2020, 31 (9), 1896–1902. [PubMed: 32799534]

64. Schmitt ND; Berger JM; Conway JB; Agar JN, Increasing Top-Down Mass Spectrometry Sequence Coverage by an Order of Magnitude through Optimized Internal Fragment Generation and Assignment. Anal. Chem 2021, 93 (16), 6355–6362. [PubMed: 33844516]

65. Zenaidee MA; Wei B; Lantz C; Wu HT; Lambeth TR; Diedrich JK; Ogorzalek Loo RR; Julian RR; Loo JA, Internal Fragments Generated from Different Top-Down Mass Spectrometry Fragmentation Methods Extend Protein Sequence Coverage. J. Am. Soc. Mass Spectrom 2021, 32 (7), 1752–1758. [PubMed: 34101447]

66. Wei B; Zenaidee MA; Lantz C; Ogorzalek Loo RR; Loo JA, Towards understanding the formation of internal fragments generated by collisionally activated dissociation for top-down mass spectrometry. Anal. Chim. Acta 2022, 1194, 339400. [PubMed: 35063165]

67. Wei B; Zenaidee MA; Lantz C; Williams BJ; Totten S; Ogorzalek Loo RR; Loo JA, Top-down mass spectrometry and assigning internal fragments for determining disulfide bond positions in proteins. The Analyst 2023, 148 (1), 26–37.

68. Li H; Sheng Y; Mcgee W; Cammarata M; Holden D; Loo JA, Structural Characterization of Native Proteins and Protein Complexes by Electron Ionization Dissociation-Mass Spectrometry. Anal. Chem 2017, 89 (5), 2731–2738. [PubMed: 28192979]

69. Li H; Nguyen HH; Ogorzalek Loo RR; Campuzano IDG; Loo JA, An integrated native mass spectrometry and top-down proteomics method that connects sequence to structure and function of macromolecular complexes. Nat. Chem 2018, 10 (2), 139–148. [PubMed: 29359744]

70. Rolfs Z; Smith LM, Internal Fragment Ions Disambiguate and Increase Identifications in Top-Down Proteomics. J. Proteome Res 2021, 20 (12), 5412–5418. [PubMed: 34738820]

71. Chin S; Chen T; Hannoush RN; Crittenden CM, Tracking internal and external ions for constrained peptides leads to enhanced sequence coverage and disulfide bond deciphering. J. Pharm. Biomed. Anal 2021, 195, 113893. [PubMed: 33445001]

72. Shukla AA; Hubbard B; Tressel T; Guhan S; Low D, Downstream processing of monoclonal antibodies—Application of platform approaches. Journal of Chromatography B 2007, 848 (1), 28–39.

73. Clauser KR; Baker P; Burlingame AL, Role of Accurate Mass Measurement (±10 ppm) in Protein Identification Strategies Employing MS or MS/MS and Database Searching. Analytical Chemistry 1999, 71 (14), 2871–2882. [PubMed: 10424174]

74. Marty MT; Baldwin AJ; Marklund EG; Hochberg GKA; Benesch JLP; Robinson CV, Bayesian Deconvolution of Mass and Ion Mobility Spectra: From Binary Interactions to Polydisperse Ensembles. Analytical Chemistry 2015, 87 (8), 4370–4376. [PubMed: 25799115]

75. Alt N; Zhang TY; Motchnik P; Taticek R; Quarmby V; Schlothauer T; Beck H; Emrich T; Harris RJ, Determination of critical quality attributes for monoclonal antibodies using quality by design principles. Biologicals 2016, 44 (5), 291–305. [PubMed: 27461239]

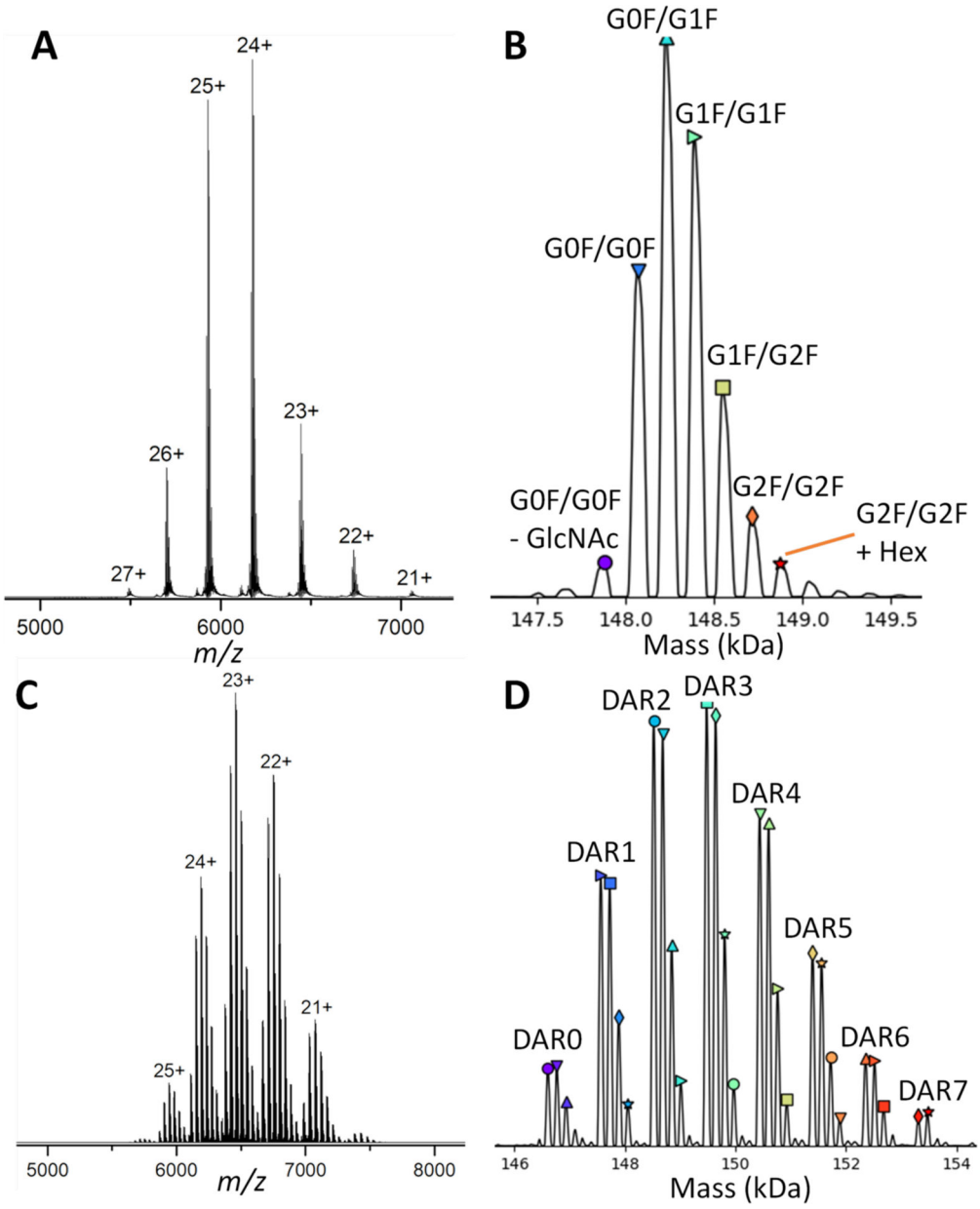

Figure 1.

(A) Native MS spectrum of the intact NIST mAb. (B) Deconvoluted zero-charged spectrum of the intact NIST mAb showing its major glycoforms.[74] (C) Native MS spectrum of the intact IgG1-DM1 ADC. (D) Deconvoluted zero-charged spectrum of the intact IgG1-DM1 ADC showing its drug distribution profile.

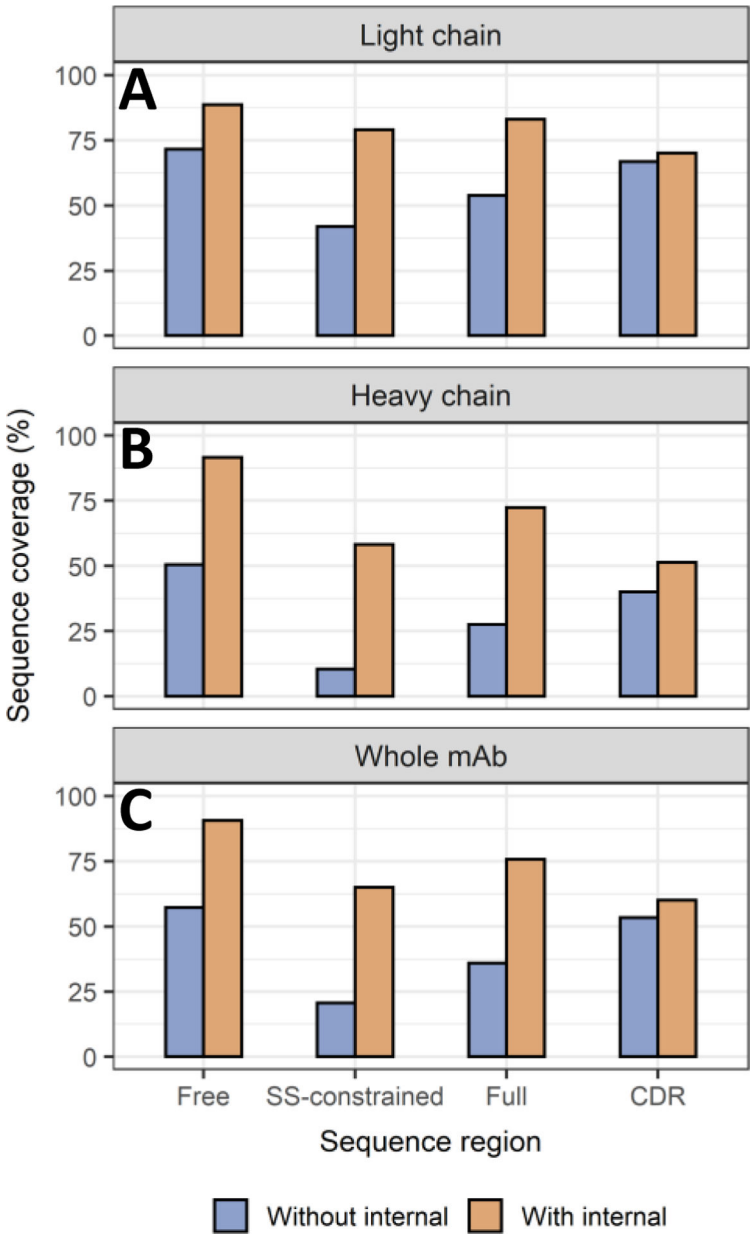

Figure 2.

Sequence coverage of different sequence regions including non-disulfide constrained sequence (“Free”), disulfide constrained sequence (“SS-constrained”), whole sequence (“Full”), and CDR sequence (“CDR”) before and after considering internal fragments of (A) light chain, (B) heavy chain, and (C) whole mAb.

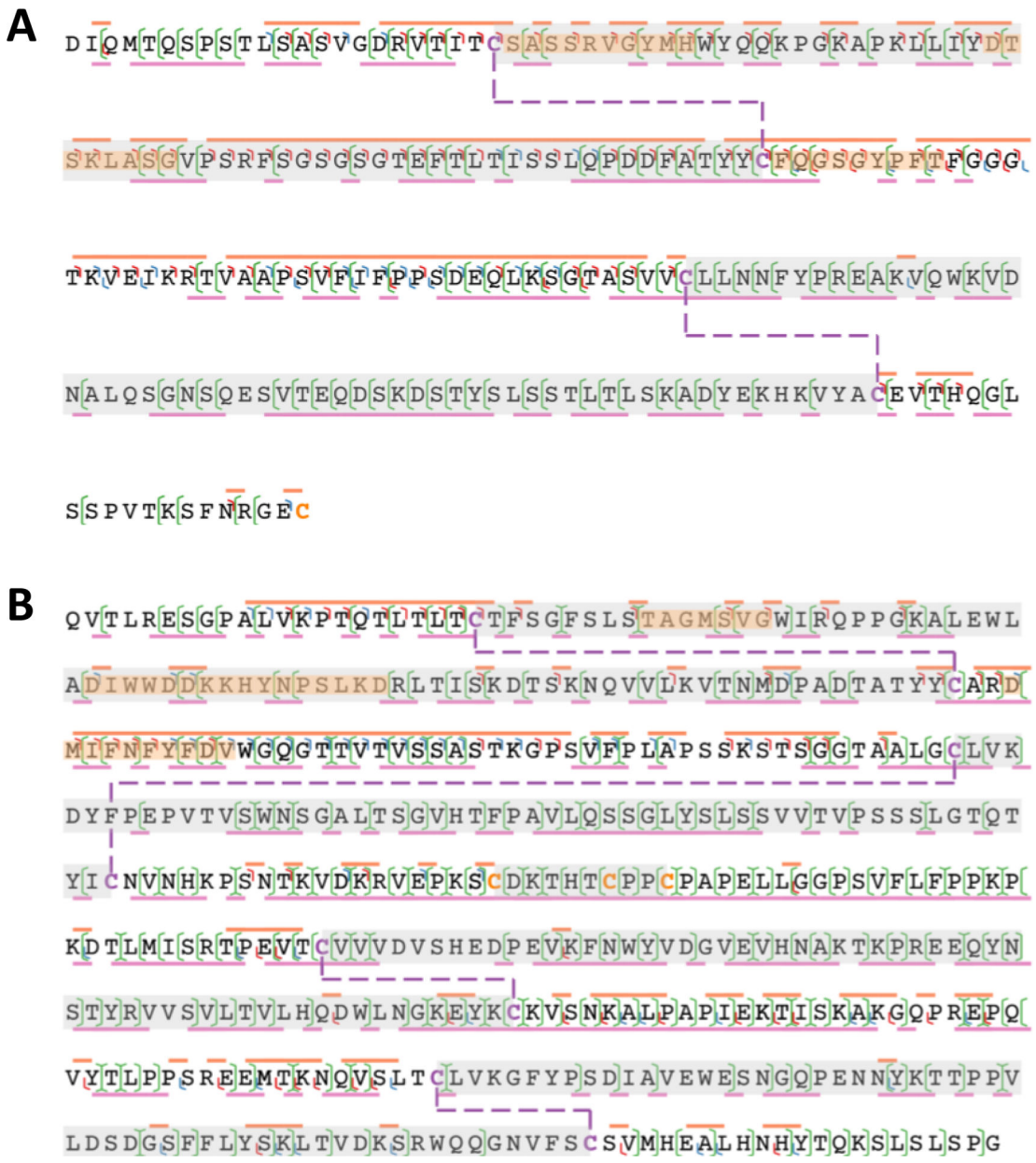

Figure 3.

Sequence coverage maps for (A) light chain and (B) heavy chain. Blue, red and green cleavages on the protein backbone represent *b*/*y*, *c*/*z*·, and *by*/*cz*· fragments, respectively. The solid line above the sequence represents terminal fragment sequence coverage, while the solid line beneath the sequence represents internal fragment sequence coverage. The purple dashed lines represent intra-chain disulfide bonds, with the sequence region constrained by disulfide bonds covered in light grey, and complementarity-determining regions (CDRs) covered in orange.

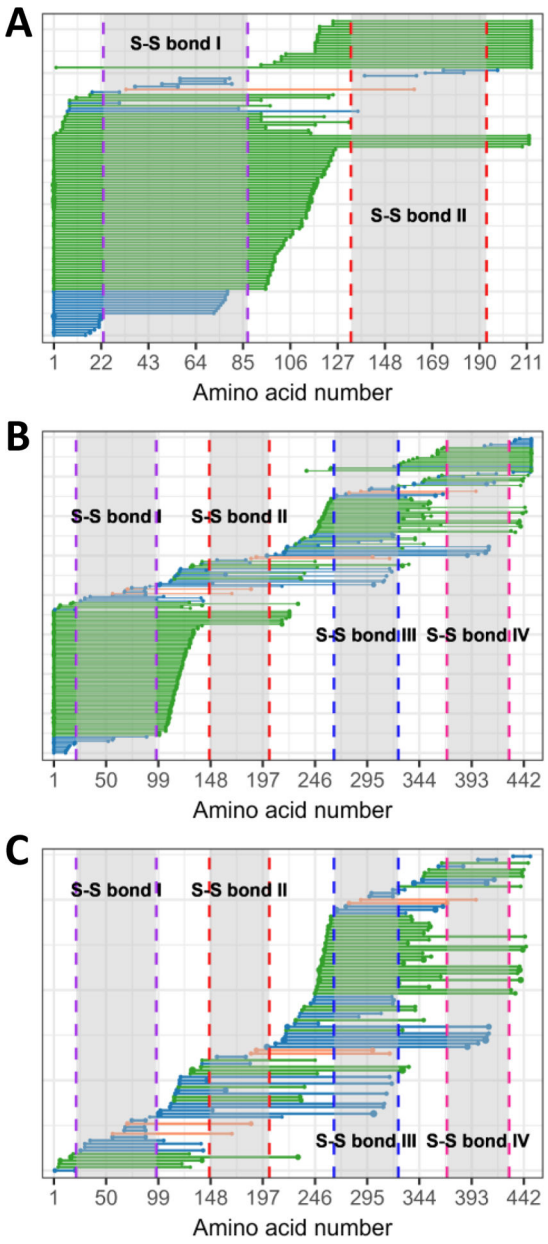

Figure 4.

Fragment location maps generated by HCD TD-MS of (A) light chain, (B) heavy chain, and (C) heavy chain with only internal fragments of intact NIST mAb after applying one hydrogen loss on each cysteine forming intra-chain disulfide bonds to indicate the integrity of the disulfide bond. Vertical dashed lines represent cysteine positions, with the same color corresponding to an intra-chain disulfide bond formed between those two cysteines. Green horizontal lines indicate fragments that can determine S-S connectivity, orange horizontal lines indicate fragments that cause mismatched dehydrocysteines, and blue horizontal lines indicate fragments that are irrelevant of S-S connectivity determination.

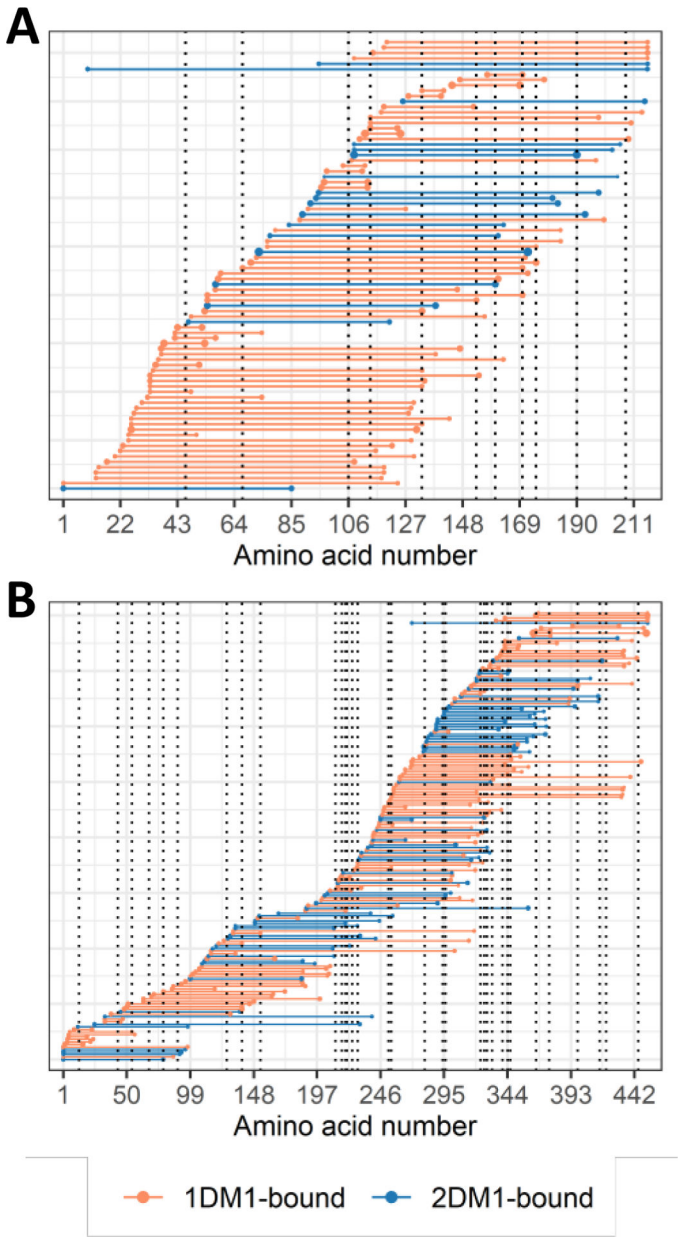

Figure 5.

Fragment location maps generated by ECD and HCD TD-MS of (A) light chain and (B) heavy chain of the intact IgG1-DM1 ADC. Black vertical dotted lines represent lysine positions. Orange and blue horizontal solid lines represent DM1-bound fragments.